Direct Measurements of Sediment Response to Waves with "Smart Sediment Grains"

Donya Frank*, Diane Foster†, Pai Chou‡, Yu-Min Kao§, Joseph Calantoni¶ and In-Mei Sou‖

*Center of Ocean Engineering, The University of New Hampshire, Durham, NH. USA. Email: donya.frank@unh.edu

†Dept. of Mechanical Engineering, The University of New Hampshire, Durham, NH. USA. Email: diane.foster@unh.edu

‡Dept. of Electrical Engineering and Computer Sc., The University of California Irvine, Irvine, CA. USA. E-mail: pai.chou@uci.edu

§Dept. of Computer Sc., National Tsing Hua University, Hsinchu, Taiwan. Email: kkming761128kk@gmail.com

¶Marine Geosciences Div., Naval Research Laboratory, Stennis Space Center, MS. USA. E-mail: joe.calantoni@nrlssc.navy.mil

‖Marine Geosciences Div., Naval Research Laboratory, Stennis Space Center, MS. USA. E-mail: InMei.Sou.ctr.pt@nrlssc.navy.mil

***Abstract*—Measurements of sediment motion have been primarily limited to indirect observations with acoustic and optical instruments. A micro-electro-mechanical systems device that can measure and record Lagrangian observations of coastal sediments at incipient motion has been developed. These sensors move freely, measure acceleration in the six degrees of freedom and their mobility characteristics are similar to coarse gravel. Experiments conducted in a small oscillating flow tunnel and a large wave flume verified that the sensors detect incipient motion under various hydrodynamic conditions. Analysis of complementary fluid velocity measurements suggest the influence of pressure gradient induced sediment motion.**

I. Introduction

Understanding the dynamics of incipient motion is extremely important because it is the small-scale process that preceeds every beach and bathymetric morphologic change which in turn impacts navigation and other larger-scale processes such as beach erosion, the stability of coastal infrastructure and wave energy dissipation. However, direct measurements of sediment at incipient motion were previously limited to Eulerian observations which were difficult to deploy at the bed without disturbing the flow. The Smart Sediment Grain (SSG) is a newly developed sensor which was tested in small and field-scale wave flumes to directly measure sediment movement at incipient motion in response to waves in the nearshore.

A. Previous Efforts

In-situ observations of sediment motion in the nearshore have been previously limited to optical and acoustic instruments which provided measurements in the wave bottom boundary layer. These flow velocity and bed evolution measurements have been used to formulate empirical sediment transport formulations.

The steady flow laboratory experiments of [1] assessed the impacts of sediment characteristics on bedload transport at incipient motion in steady flow. These results have been used to formulate the Shields parameter, θ, which parameterizes the force required to move a single exposed sediment grain. The data suggested that sediment motion results from the destabilizing force of the shear stress. The critical Shields parameter for sediment motion was determined to be roughly 0.05, suggesting the shear stress gradient needs to exceed 5% of the immersed weight of the grain to trigger sediment motion. Numerical models ([2]–[6]) and laboratory experiments ([7]–[9]) also suggested that the shear stress is predominantly responsible for sediment motion.

However, more recently it has been shown that the pressure gradients in the flow may also initiate sediment motion and [10] quantified these effects with the Sleath parameter (S) by balancing the inertial and gravitational forces acting on the grains. Bed mobilizations occured above a critical S of 0.29. Field observations by ([11]) also detected sediment motion under peak pressure gradients during the strengthening of onshore-directed flow. Sediment transport was initiated during the large accelerations ($\geq$ 200 cm/s^2) present during flow reversal from offshore- to onshore-directed flow. Calculated Sleath values during the bed mobilizations yielded a threshold value of 0.08-0.1. This suggests a lower critical limit for natural beds exposed to surface gravity waves compared to laboratory experiments with a rigid lid. The bed mobilizations was assumed to result from pressure gradient forcing because they did not occur during peaks in the Shields parameter.

Accurately assessing the fluid mechanisms that trigger sediment motion requires highly detailed in-situ direct measurements at the fluid-sediment interface. In-situ Eulerian measurements of bed-shear stresses have been made with shear plates ([9], [12]). However, they are difficult to deploy in the thin mobile bed layer and field environments. Other in-situ measurements within the wbbl include field observations of velocity with hot-film anemometers ([13]), Acoustic Doppler Velocimeters (ADV's) ([14], [15]) and Laser Doppler Velocimeters ([16]). Particle Image Velocimetry has also been used to observe the fluid-sediment interaction within the wbbl ([17], [18]) but are unable to perform Lagrangian measurements and are difficult to deploy in the field. Moreover, signal attenuation severely limits measurements within the mobile bed layer.

With the recent advancements in multi-axis force measurement technology and low-power wireless embedded systems, a Lagrangian method for performing direct measurements of the movement of grains has now been developed. In-situ measurements of sediment transport were made with new state-of-the-art micro-electronic machines (MEM's). These sensors

978-0-933957-40-4 ©2013 MTS

were used to measure the response of gravel-sized sediment to various wave conditions.

B. Objectives

The goal of this effort is to enhance the scientific community's understanding of the hydrodynamics and morphodynamics within the wave-dominated bottom boundary layer through the assessment of the mechanisms that trigger incipient motion and the small-scale fluid-sediment interactions at the bed. This paper describes the characteristics of the smart sediment grain (SSG) as an autonomous sensor for the Lagrangian detection of inicpient motion under oscillatory flows. They have been deployed in both small and large scale wave flumes. Sample data sets with preliminary analyses are presented here.

II. The Sensor

The sensors weigh 4 grams and measure 2.5x1.5x1.4 cm each. They are equipped with 2 tri-axial accelerometers, a flash memory card for onboard data storage, a battery and wireless transmitter, Figure 1a. The accelerometers can be programmed to sense at 2, 4 and 8 times the gravitational acceleration (g) to improve range, resolution and sensitivity. The use of 2 accelerometers to resolve the 6 degrees of freedom for translation and rotation in the three dimensions, instead of a gyroscope, enables the node to be one of the smallest, self-contained programmable Inertial Measurement Units (IMU's) ([19]). The sensors detect gravity, which allows for re-orientation of the accelerations from the sensor's coordinate system to real-world coordinates.

The sensor was first encased in heat shrink tubing to increase robustness before being enclosed inside a spherical Delrin plastic enclosure (Figure 1b). The Delrin enclosure is comparable in size to coarse gravel with a diameter of 4.4 cm. The SSG has a combined specific gravity of the sensor and the enclosure of 1.3. Delrin had the ideal physical and electical properties as it was easy to machine, had the appropriate density to facilitate tests in the incipient motion regime in small-scale and large-scale wave flumes and was transparent to radio frequency.

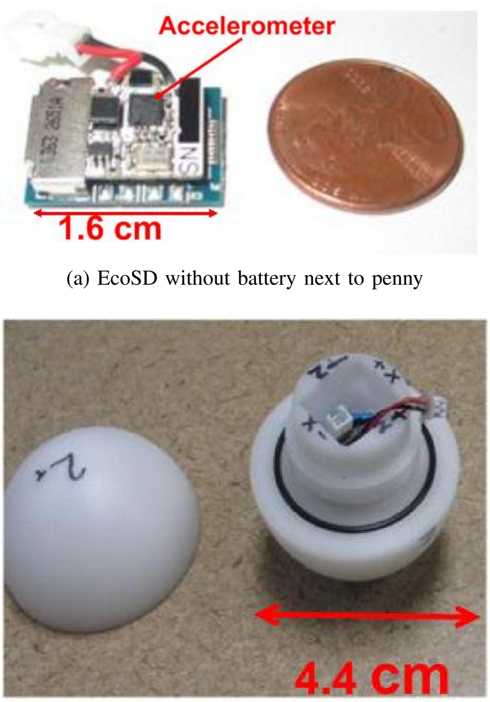

(a) EcoSD without battery next to penny

(b) EcoSD enclosed in Delrin sphere.

Fig. 1: The Smart Sediment Grain.

III. SSG Testing

Preliminary tests were conducted during the development of the SSG to determine their resolution, sensitivity, accuracy and threshold for measuring acceleration. These tests verified that the sensors were functioning properly and could accurately record the accelerations of sediment motion, not expected to exceed 2g at incipient motion.

During this evaluation phase, still tests were conducted with a commercial reference accelerometer to determine the noise floor of the accelerometers. Time domain, as well as, frequency domain analyses were conducted to determine the characteristics and limitations of the accelerometers. The noise floor of the sensors was approximately 0.5 m/s^2. This is low enough to accurately capture the accelerations at incipient motion. Based on the findings of [20], the sediment acceleration at incipient motion was approximately 0.4g or 4 m/s^2. Shaking tests at varying frequencies and amplitude were also conducted with the commercial reference accelerometer. Frequency analyses determined that the sensors accurately captured the oscillations amplitude and peak frequency components. A sampling frequency of 50 Hz was sufficient to accurately capture the wave characteristics while extending storage capacity and battery life of the sensor.

Experiments were also conducted to determine the angle of repose of the SSG with the device shown in Figure 2. The board was raised incrementally until the SSG rolled. The average angle of repose obtained was approximately 36° which agrees to within 10% of the typically reported value for coarse gravel of 40° ([21]).

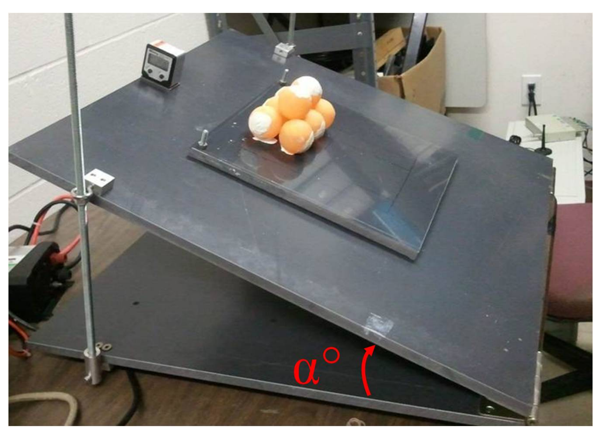

Fig. 2: Experimental setup for the angle of repose (α).

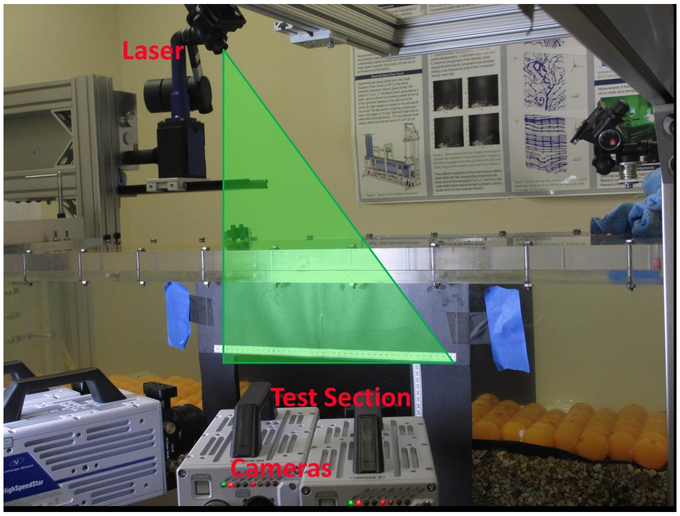

Fig. 3: Experimental setup for the small-scale wave flume tests at The Naval Research Laboratory.

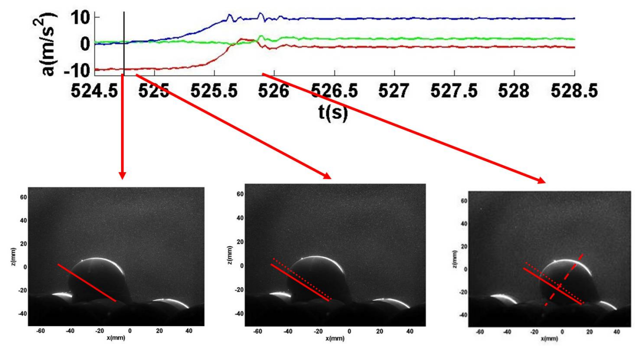

Fig. 4: SSG accelerations and PIV images at incipient motion of the SSG in flows with orbital velocity amplitude of 0.2 m/s and period of 5 s. The black vertical line indicates the onset of motion and the solid, dotted and dashed red lines highlight the position of the equatorial stripe on the ball.

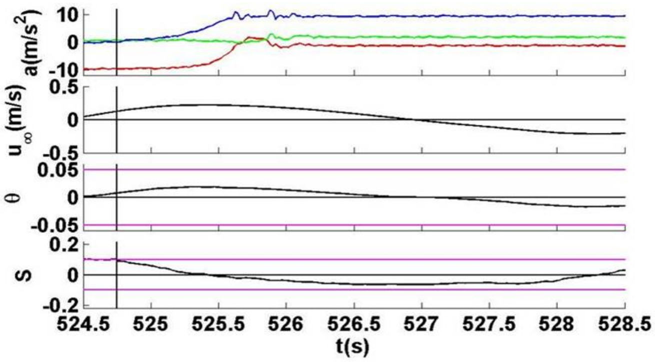

Fig. 5: Measured accelerations (top) and free stream velocities (second) at incipient motion in flows with orbital velocity amplitude of 0.2 m/s and period of 5 s in the small oscillating flow tunnel. The black vertical lines indicate the onset of motion of the SSG. The colors red, green and blue represent the x, y and z dimensions (top). The third and fourth panels show the calculated values of the Shields parameter (θ) and the Sleath parameter (s), respectively.

IV. Small-Scale Wave Flume Testing of the SSG

The SSGs were then evaluated in a small-scale flume at the OH Hinsdale Wave Research Laboratory, Oregon State University, Oregon, USA. Their behavior under various wave forcing conditions was observed in the small-scale controlled environment. The plexiglass wave flume is 0.15 m x 0.46 m x 4.9 m. Waves were generated by a manually operated spring-loaded paddle. Testing in the wave flume verified that incipient motion of the balls would occur and that the accelerometers would capture this movement. Complementary video clips were recorded during the experiment to verify the movement of the smart grains. Spectral analysis on the acceleration was performed to confirm that the sensors actually measured the motion due to the waves by indicating peak energies at the wave frequencies.

The SSG's were also deployed in the Small-Oscillating Flow Tunnel, Naval Research Laboratory. The facility is shown with the experimental setup in Figure 3. A water level sensor, stereographic and tomographic Particle Image Velocimetry (PIV) assessed the flow properties from which the shear stress and pressure gradients will be calculated. The laser and 4 high-speed cameras which comprise the PIV system are shown in Figure 3. A full range of hydrodynamic conditions were tested with orbital velocity amplitudes ranging from 0.15 m/s to 0.5 m/s and periods from 2 s to 8 s. The SSG were tested in a natural hexagonally packed manner, as well as, with a single proud grain exposed to the flow. Next, 2 exposed grains were placed 2 grain diameters apart to assess the effects of sheltering from nearby sediments on incipient motion.

Figure 4 shows SSG accelerations and PIV images from a sample data set. The white line across the top of the balls represents the laser sheet. The panels show the SSG right before it moves (left), 0.1 s after the onset of motion (center) and after it has stopped rolling (right). These images illustrate that the ball has rolled to the adjacent pocket onshore. There is a white stripe on the balls which can be visually tracked to qualitatively determine its orientation. The location of this white stripe is highlighted by the solid red line in the left image, the dotted line in the center image and as a dashed red line in the right image.

Figure 5 shows the accelerations measured by the SSG during incipient motion in the top panel. Before the SSG rolls, the gravity vector is predominantly in the -x direction in the sensor's coordinate system. When the ball rotates as it rolls, the gravity vector can be seen predominantly in the +z direction in the sensor's coordinate frame when it has stopped. The instantanaeous free stream velocities for this dataset are shown in the second panel of Figure 5 over a complete wave cycle. The vertical black lines indicate the onset of incipient motion.

Calculated values of the Shields parameter (θ) over the wave cycle are shown in the third panel of Figure 5. These values were computed with the friction factor quadratic formulation of [22]. It can be seen that θ values are below the critical threshold of 0.05 when the SSG begins to roll. This suggests that the bed shear stress may not be responsible for incipient motion of the SSG.

The Sleath parameter (S) quantifying the effects of the pressure gradients and accelerations of the flow on the sed-

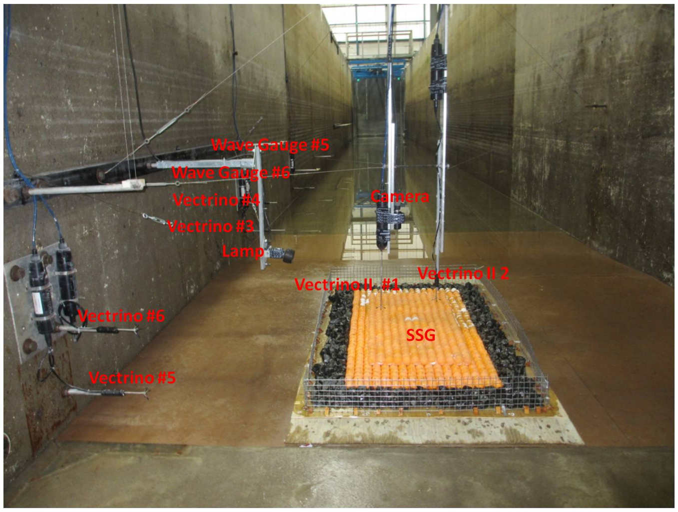

Fig. 6: Experimental setup for large-scale wave flume tests at The O.H. Hinsdale Wave Research Laboratory.

iment was formulated with

$$S = -\frac{dP}{dx}\frac{1}{(\rho_s - \rho)g} \tag{1}$$

where P is the pressure and x is the horizontal coordinate. Using Linear Wave Theory, $\frac{dP}{dx}$ can be approximated with the free-stream horizontal acceleration $-\frac{dP}{dx} = \rho\left(\frac{du_\infty}{dt}\right)$ ([11]). The onset of motion occured at the peak of the Sleath parameter(S) during the strengthening phase of the onshore directed flow, in agreement with [11], note the bottom panel of Figure 5. This suggests that for this flow, incipient motion was more likely triggered by the pressure gradients and not the bed shear stress.

V. Large-Scale Wave Flume Testing of the SSG

The SSG's were deployed at the field-scale wave flume (104 m x 3.7 m x 4.6 m) at the O.H. Hinsdale Wave Research Laboratory Oregon State University. Waves were generated by a piston-type wave paddle. The balls were first configured in a movable grid-like lattice and next with a single ball sitting proudly on top of a fixed sediment bed constructed with corn syrup-filled ping pong balls. Wave gages and ADV's measured the hydrodynamics in the test section and an underwater camera provided visual confirmation of sediment movement (Figure 6).

Figure 7 illustrates a sample data set of the large-scale experiments. The recorded accelerations indicate that the ball rocked twice before rolling 1 grain diameter to the adjacent pocket onshore, note the humps indicated by the first 2 vertical black lines.

Figure 8 shows the accelerations measured by the SSG during incipient motion in the top panel. Before the SSG rolls, the gravity vector is predominantly in the -y direction in the sensor's coordinate system. When the ball rotates as it rolls, the gravity vector can be seen predominantly in the -z direction. The instantanaeous free stream velocities for this dataset are shown in the second panel of Figure 8 over a several wave cycles. The vertical black lines highlight that the onset of sediment motion occurred during the accelerating

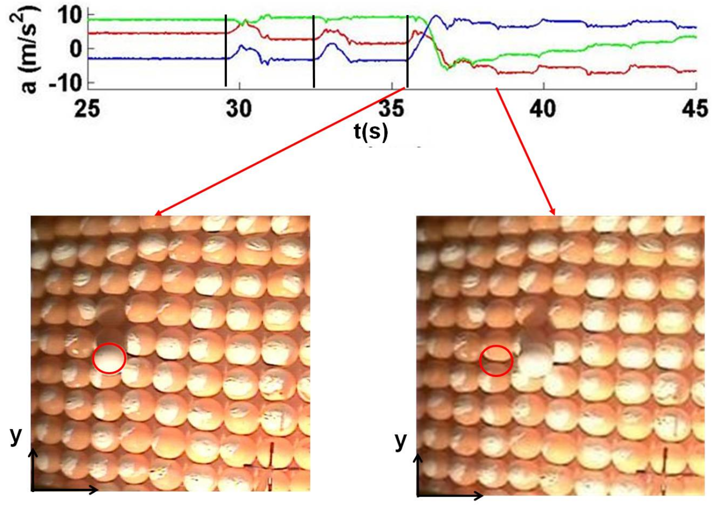

Fig. 7: Incipient motion of SSG in waves with height of 0.2 m and period of 3 s in the large wave flume. The black vertical lines indicate the onset of motion and the red circle highlights the initial position of the ball.

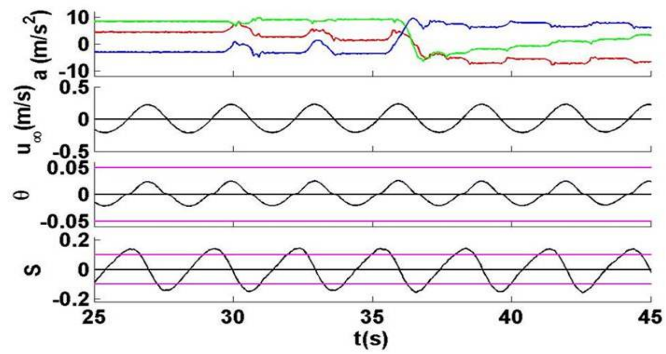

Fig. 8: Measured accelerations (top) and free stream velocities (second) at incipient motion in flows with orbital velocity amplitude of 0.2 m/s and period of 5 s in the large wave flume. The black vertical lines indicate the onset of motion of the SSG. The colors red, green and blue represent the x, y and z dimensions. The third and fourth panels show the calculated values of the Shields parameter (θ) and the Sleath parameter (s), respectively.

onshore phase of the wave cycle and also correspond well with the peaks in the Sleath parameter estimates. Once again, suggesting that the pressure gradients were responsible for sediment motion, and not the bed shear stresses. Note that the Shields parameter estimates were well below the critical threshold when the SSG moved.

VI. Summary

An autonomous sensor has been developed to conduct Lagrangian measurements of sediment response to wave forcing. Preliminary testing of the SSG verified that they have a low noise floor and their enclosures are electronically transparent. Angle of repose experiments verified that the mobility of the SSG is similar to coarse gravel. Small-scale testing for the development of the smart grain confirmed that incipient motion of the Delrin plastic enclosures occurs, was captured by the accelerometers and verified by the recorded video.

Preliminary analyses suggest evidence of pressure-gradient influenced motion in both small and large scale wave flumes experiments. Further work includes more detailed analyes of these datasets and comparisons with other types of sediments.

ACKNOWLEDGMENT

We would like to thank The National Science Foundation for funding, as well as, our collaborators and colleagues for their support and advice.

REFERENCES

[1] A. Shields, "Anwendung der anhlichkeitsmechanik und turbulenzforschung auf die geschiebebewegung." *Mitt Preuss Versuchsanstalt fur Wassebau und Schiffbau.*, vol. 26, 1936.

[2] A. G. Davies, R. L. Soulsby, and H. L. King, "A numerical model of the combined wave and current bottom boundary layer." *J. Geophys. Res.*, vol. 93, no. C1, pp. 491–508, January 1988.

[3] W. D. Grant and O. S. Madsen, "Combined wave and current interaction with a rough bottom," *J. Geophys. Res.*, vol. 84, no. C4, pp. 1,797–1,808, April 1979.

[4] O. Madsen and P. Wikramanayake, "Simple models for turbulent wave-current bottom boundary layer flow." Mass. Inst. Tech. Ralph M. Parsons Lab., Cambridge, Mass., Tech. Rep., 1991.

[5] R. L. Soulsby and S. Clarke, "Bed shear-stresses under combined waves and currents on smooth and rough beds." Tech. Rep., August 2005.

[6] R. Styles and S. M. Glenn, "Modeling stratified wave and current bottom boundary layers on the continental shelf," *J. Geophys. Res.*, vol. 24, pp. 24,119–24,139, 2000.

[7] H. Afzalimhr, S. Dey, and P. Rasoulianfar, "Influence of decelerating flow on incipient motion of a gravel-bed stream," *Journal of Sādhanā, Engineering Sciences, Indian Academy of Sciences*, vol. 32, no. 5, pp. 545–559, 2007.

[8] D. Huntley and D. Hazen, "Seabed stressed in combined wave and steady flow conditions on the nova scotia continental shelf: field measurements and predictions." *Am. Met. Soc.*, vol. 18, pp. 347–362, 1988.

[9] K. L. Rankin and R. I. Hires, "Laboratory measurement of bottom shear stress on a movable bed." *J. Geophys. Res.*, vol. 105, no. C7, pp. 17 011–17 019, 2000.

[10] J. F. A. Sleath, "Conditions for plug formation in oscillatory flow," *Cont. Shelf Res.*, vol. 19, no. 13, pp. 1,643–1,664, October 1999.

[11] D. L. Foster, A. J. Bowen, and R. A. Holman, "Field evidence of pressure gradient induced incipient motion," *J. Geophys. Res.*, vol. 111, no. C5, C05004, pp. 1–8, 2006.

[12] J. Kamphuis, "Friction factor under oscillatory waves." *J. of Waterway, Port and Ocean Div.*, vol. 101, no. WW2, pp. 135–144, 1975.

[13] D. L. Foster, R. A. Beach, and R. A. Holman, "Field observations of the wave bottom boundary layer," *J. Geophys. Res.*, vol. 105, no. C8, 2000.

[14] C. R. Sherwood, J. R. Lacy, and G. Voulgaris, "Shear velocity estimates on the inner shelf off grays harbor, washington, usa," *Cont. Shelf Res.*, vol. 26, pp. 1995–2018, 2006.

[15] C. Smyth and A. Hay, "Wave friction factors in nearshore sands." *J. of Phys. Ocean.*, vol. 32, pp. 3490–3498, 2002.

[16] J. H. Trowbridge and Y. C. Agrawal, "Glimpses of a wave boundary layer," *J. Geophys. Res.*, vol. 100, no. C10, pp. 20,729–20,743, October 1995.

[17] H. C. Earnshaw, "A study of flow over a rippled bed using particle image velocimetry." Ph.D. dissertation, Univ. of Edinburgh, UK., 1996.

[18] C. S. Nichols and D. L. Foster, "Full-scale observations of wave-induced vortex generation over a rippled bed," *J. Geophys. Res.*, vol. 112, 2007.

[19] C. Park and P. Chou, "Eco: Ultra-wearable and expandable wireless sensor platform." in *Proc. 3rd Int. Workshop on Body Sensor Networks, MIT Media Lab.*, Cambridge, MA, USA., 2006.

[20] J. Calantoni, K. T. Holland, and T. G. Drake, "Modelling sheet-flow sediment transport in wave-bottom boundary layers using discrete-element modelling." *Philosophical Transactions of The Royal Society of London.*, vol. A, no. 362, 2004.

[21] P. Y. Julien, *Erosion and Sedimentation*, 1st ed. Cambridge University Press, 1994.

[22] D. Myrhaug, "A rational approach to wave friction coefficients for rough, smooth and transitional turbulent flow," *Coast. Eng.*, vol. 13, no. 1, pp. 11–21, 1989.